OPEN ACCESS

Japanese Journal of Applied Physics **61**, 118001 (2022) **BRIEF NOTE**

https://doi.org/10.35848/1347-4065/ac9810

Temperature sensing based on multimode interference in polymer optical fibers: sensitivity enhancement by PC-APC connections

Kun Wang[1,2*], Yosuke Mizuno[2], Kazuya Kishizawa[2], Yuma Toyoda[2], Heeyoung Lee[3], Koichi Ichige[2], Wolfgang Kurz[1,2], Xingchen Dong[1], Martin Jakobi[1], and Alexander W. Koch[1]

[1]*Institute for Measurement Systems and Sensor Technology, Department of Electrical and Computer Engineering, Technical University of Munich, Arcisstraße 21, Munich D-80333, Germany*

[2]*Faculty of Engineering, Yokohama National University, 79-5 Tokiwadai, Hodogaya-ku, Yokohama 240-8501, Japan*

[3]*College of Engineering, Shibaura Institute of Technology, 3-7-5 Toyosu, Koto-ku, Tokyo 135-8548, Japan*

[*]E-mail: kun88.wang@tum.de

Received August 24, 2022; revised September 15, 2022; accepted October 5, 2022; published online October 18, 2022

A simple, stable, and high-sensitivity temperature sensor based on multimode interference in a polymer optical fiber (POF) with higher-order mode excitation has been developed. In a single-mode–multimode–single-mode (SMS) structure, one end of the multimode POF with physical-contact (PC) connectors is connected to a silica single-mode fiber with an angled-PC (APC) connector. We compare the temperature sensing characteristics of the three configurations (no PC-APC, PC-APC at input, and PC-APC at output) and obtain the highest temperature sensitivity of 219.2 pm °C^{-1}, which is more than double the value of the standard (no PC-APC) SMS structure. © 2022 The Author(s). Published on behalf of The Japan Society of Applied Physics by IOP Publishing Ltd

Fiber-optic temperature sensors have intrinsic characteristics, such as compact size, lightweight, fast response, remote sensing capabilities, and insensitivity to ambient electromagnetic fields.[1–5] Various fiber-optic temperature sensors have been developed by exploiting fiber Bragg gratings (FBGs),[6,7] long-period gratings (LPGs),[8] Brillouin scattering,[9] Raman scattering,[10] and surface plasmon resonance.[11] Each technique has its own advantages and disadvantages; some of these techniques suffer from sophisticated equipment, high cost, and/or fabrication complexity. One simple and low-cost implementation based on the multimode interference (MMI) effect is a so-called single-mode–multimode–single-mode (SMS) fiber sensor.[12] Many SMS-based configurations implementing silica optical fibers have been reported for various sensing scenarios.[13–19]

In addition to silica optical fibers, polymer optical fibers (POFs) have also been used for sensing applications.[20–23] Although the optical attenuation of a POF is higher than that of silica optical fibers, its influence is sometimes negligible for a short POF. Compared to conventional silica optical fibers, POFs have some unique properties such as higher strain limits, biocompatibility, higher fracture toughness, and flexibility in bending.[24] In 2012, Huang et al. employed a POF, which was a 0.16 m long step-index POF made of a polymethyl methacrylate, in the SMS-based temperature sensor and obtained a temperature sensitivity of 56.8 pm °C^{-1}.[25] Since then, SMS-based temperature sensing has been extensively studied. The sensing performance of a perfluorinated (PF) graded-index (GI) POF, which has relatively low loss at 1300 nm, was investigated in 2014. With a length of 1.0 m and a core diameter of 120 μm, a temperature sensitivity of 0.74 pm °C^{-1} was achieved at room temperature at 1300 nm.[26] Later, the PFGI-POF was tested when the temperature increased close to the glass-transition temperature of the core polymer (~70 °C). Furthermore, a significantly improved temperature sensitivity of 202 nm °C^{-1}, with a length of 1.0 m and a core diameter of 62.5 μm, was obtained at 72 °C at 1300 nm.[27] In 2017, the impact of annealing a POF on the temperature sensitivity at room temperature was studied. Compared to the temperature sensitivity without annealing, the sensitivity was enhanced 2.9 times by annealing the POF at 90 °C.[28]

In this work, we develop an extremely simple and stable POF-based SMS temperature sensor with physical-contact (PC)-to-angled-PC connection for making use of higher-order modes in the POF. One end of a 50 cm long POF is connected to an SMF via an APC/PC adaptor (from an 8° angle-polished APC connector to a 0° PC connector or the reverse) to exploit the higher-order propagation modes in the POF. This scheme exhibits high stability because of the accurately fabricated commercial adaptors and connectors. A comparison experiment of three different configurations (no PC-APC, PC-APC at input, and PC-APC at output) is carried out, and the highest temperature sensitivity is >2 times that of the perfectly aligned SMS structure. This result indicates that the temperature sensitivity can be improved by the use of higher-order modes induced by PC-APC connections.

The sensing principle is based on the MMI effect in the SMS structure. The injected light is guided through the input SMF into the multimode fiber (MMF) section, and the first few modes in the MMF are excited, which is induced by the spot-size difference between the fundamental modes in the SMF and MMF. At the second conjunction of the MMF/SMF, these modes are coupled back to the fundamental mode of the output SMF. The power in the output SMF (P_{out}) can be given as[29,30]

$$P_{\mathrm{out}} = |A_0^2 + A_1^2\, e^{i(\beta_0-\beta_1)L} + A_2^2\, e^{i(\beta_0-\beta_2)L} + \ldots|^2, \quad (1)$$

where A_i is the field amplitude of the ith mode at the first SMF/MMF boundary, β_i is the propagation constant of the ith mode, and L is the length of the MMF. It is clear that P_{out} is affected by the temperature applied to the MMF, influencing β_i and L. Therefore, temperature sensing can be performed by measuring the shifts in terms of either power or spectral location of peaks (or dips).

However, this principle holds true only when the MMF and two SMFs are perfectly aligned. When they are misaligned, e.g.,

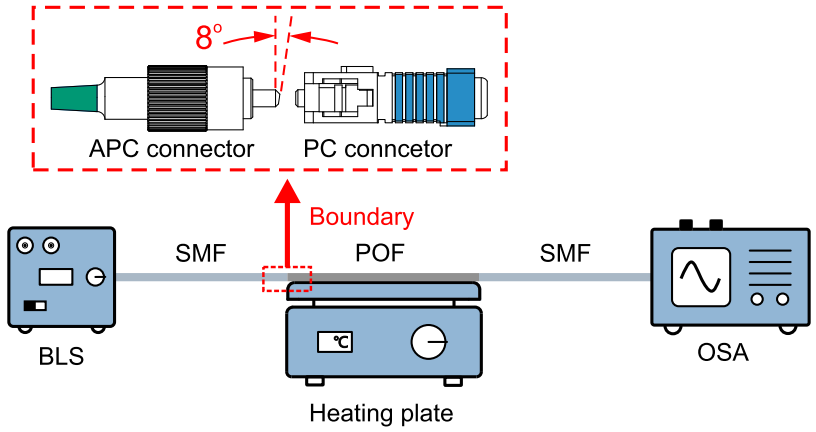

Fig. 1. (Color online) Schematic diagram of the experimental setup and the sensor configuration. The inset shows the APC/PC connection at the SMF/POF boundary. BLS, broadband light source; SMF, single-mode fiber; POF, polymer optical fiber; and OSA, optical spectrum analyzer.

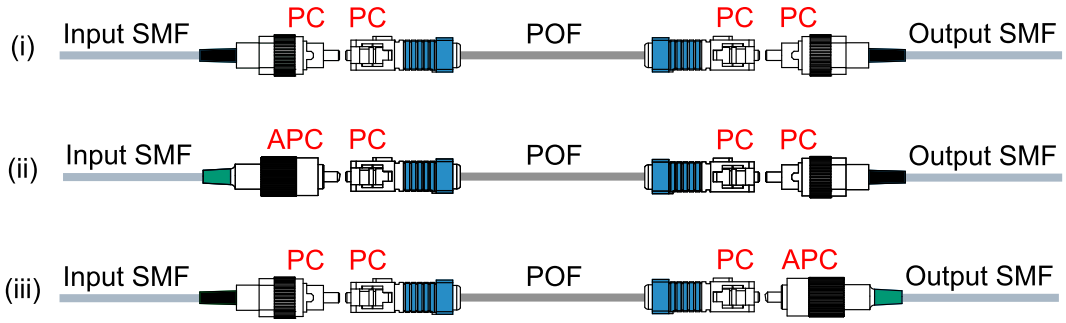

Fig. 2. (Color online) Schematic diagrams of the different sensor configurations: (i) SMF-PC/PC-POF-PC/PC-SMF, (ii) SMF-APC/PC-POF-PC/PC-SMF, and (iii) SMF-PC/PC-POF-PC/APC-SMF.

offset SMS structure, there is potential that a larger number of higher-order modes are excited. It is natural to assume that the excitation of higher-order modes may lead to an improvement in sensitivity. To verify this assumption, we introduce the use of PC-APC connections at the SMF/POF boundaries in the SMS structure to exploit higher-order modes in the POF.

The schematic diagram of the experimental setup is shown in Fig. 1. Both ends of a 50 cm long PFGI-POF[31] are coupled to the ends of two silica SMFs (size: 9/125 μm) by PC/PC or APC/PC connections. This POF has a three-layered structure of core, cladding, and over-cladding (diameters: 50, 70, and 490 μm; refractive indices: ∼1.35, ∼1.34, and 1.59, respectively). The materials of the core/cladding layers and the over-cladding layer are doped/undoped amorphous perfluorinated polymers and polycarbonate, respectively. The numerical aperture is 0.185, and the propagation loss at 1550 nm is ∼0.25 dB m^{-1}. The proximal end of the input SMF is connected to a broadband light source (ASE-FL7002, Thorlabs) emitting the incident light, while the distal end of the output SMF is connected to an optical spectrum analyzer (OSA), which detects the changes in the transmitted light spectrum. The POF Section is placed straight on a heating plate during the measurement. Three configurations, as depicted in Fig. 2, are tested: (i) SMF-PC/PC-POF-PC/PC-SMF, (ii) SMF-APC/PC-POF-PC/PC-SMF, and (iii) SMF-PC/PC-POF-PC/APC-SMF. Hereafter, these structures will be referred to as Config. (i), Config. (ii), and Config. (iii). The POF has two subscriber-connector (SC)/PC connectors, and the SMFs have ferrule connector (FC)/PC or FC/APC connectors. The PC connector has a polished flat end, while the APC connector contains an 8° angle polished end. The high Fresnel reflection at the PC/APC boundary does not significantly influence the measured results, because the spectrum of not reflected but transmitted light is observed in this configuration.

The temperature experiments with these configurations were performed under the same condition in the range of 40 °C–50 °C in steps of 2 °C. As shown in Figs. 3(a)–3(c), the spectral dips exhibited redshifts in the wavelength domain when the temperature increased for Config. (i), Config. (ii), and Config. (iii). The corresponding wavelength shifts of the spectral dips against the temperature variations are plotted and fitted in Figs. 3(d)–3(f). The temperature sensitivities are calculated to be 98.4 pm °C^{-1} [Config. (i)], 136.1 pm °C^{-1} [Config. (ii)], and 219.2 pm °C^{-1} [Config. (iii)]. The result proves that the use of PC-APC connections improves the sensitivity, and the maximal temperature sensitivity of Config. (iii) is >2 times the value of Config. (i). Note that the experiment of Config. (iii) was repeated several times after disconnecting and re-connecting the APC-PC boundary, which led to almost the same sensitivities with changes of <1%. Simply thinking, the PC-APC connection on the input side will excite a larger number of higher-order propagation modes in the POF than that on the output side, but the measured sensitivity is lower. The physical reason for this behavior is unknown yet (note that all the previously established theories on the operation of an SMS structure were derived under the assumption that all the modes are axially symmetrical). As the fabrication technique of this POF is relatively immature and its uniformity is low compared to silica fibers, a large number of higher-order modes may be intrinsically excited in a POF, some of which may be promoted to be coupled to the output SMF by the PC-APC connection on the output side. Further study is required on this point.

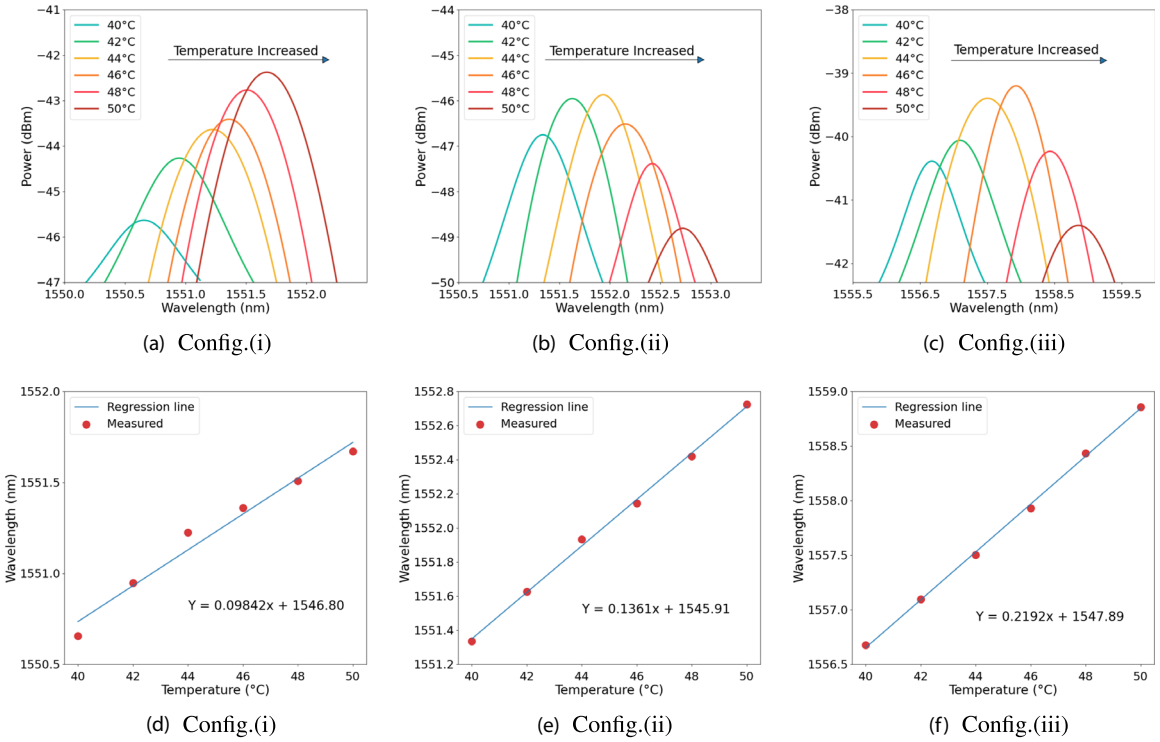

Fig. 3. (Color online) Temperature measurement results for different configurations. Measured spectral dependencies on temperature: (a) Config. (i), (b) Config. (ii), (c) Config. (iii). Spectral dip shifts plotted as a function of temperature: (d) Config. (i), (e) Config. (ii), and (f) Config. (iii).

In conclusion, we succeeded in doubling the sensitivity of a POF-MMI-based temperature sensor by the simple use of PC-APC connections. Compared to other methods for exciting higher-order modes, this structure has higher stability due to the precisely fabricated commercial connectors. Three configurations, including SMF-PC/PC-POF-PC/PC-SMF, SMF-APC/PC-POF-PC/PC-SMF, and SMF-PC/PC-POF-PC/APC-SMF, were experimentally studied. The measurement result shows that using PC-APC connections enhances the temperature sensitivity, and the maximum temperature sensitivity of 219.2 pm $°C^{-1}$ is more than double the value for the standard configuration. Thus, we believe this work will be of significant use as a simple and stable method for enhancing the sensitivity of SMS-based temperature sensors.

Acknowledgments The authors would like to thank the China Scholarship Council (CSC) (Grant No. 201808340074) for supporting this work. Y.M. and H.L. are indebted to the Japan Society for the Promotion of Science (JSPS) KAKENHI (Grant Nos. 21H04555 and 22K14272), and the research grants from the Murata Science Foundation, the Telecommunications Advancement Foundation, the Takahashi Industrial and Economic Research Foundation, the Yazaki Memorial Foundation for Science and Technology, and the Konica Minolta Science and Technology Foundation.

ORCID iDs Kun Wang https://orcid.org/0000-0003-0410-204X Yosuke Mizuno https://orcid.org/0000-0002-3362-4720 Heeyoung Lee https://orcid.org/0000-0003-3179-0386

1) X. Wang and O. S. Wolfbeis, Anal. Chem. **92**, 397 (2020).
2) A. Leung, P. M. Shankar, and R. Mutharasan, Sensors Actuators B **125**, 688 (2007).
3) Y. Mizuno, G. Numata, T. Kawa, H. Lee, N. Hayashi, and K. Nakamura, IEICE Trans. Electron. **E101.C**, 602 (2018).
4) K. Wang, X. Dong, M. H. Köhler, P. Kienle, Q. Bian, M. Jakobi, and A. W. Koch, IEEE Sens. J. **21**, 132 (2021).
5) S. Pevec and D. Donlagić, Opt. Eng. **58**, 1 (2019).
6) B.-O. Guan, H.-Y. Tam, X.-M. Tao, and X.-Y. Dong, IEEE Photon. Technol. Lett. **12**, 675 (2000).
7) D. J. Webb, Meas. Sci. Technol. **26**, 092004 (2015).
8) C.-L. Zhao, L. Xiao, J. Ju, M. S. Demokan, and W. Jin, J. Lightwave Technol. **26**, 220 (2007).
9) Y. Mizuno, N. Hayashi, H. Fukuda, K. Y. Song, and K. Nakamura, Light Sci. Appl. **5**, e16184 (2016).
10) M. N. Alahbabi, Y. T. Cho, and T. P. Newson, Opt. Lett. **30**, 1276 (2005).
11) Y. Wang, Q. Huang, W. Zhu, M. Yang, and E. Lewis, Opt. Express **26**, 1910 (2018).
12) D. Donlagic and B. Culshaw, J. Lightwave Technol. **17**, 1856 (1999).
13) Y. Gong, T. Zhao, Y.-J. Rao, and Y. Wu, IEEE Photon. Technol. Lett. **23**, 679 (2011).
14) A. B. Socorro, I. D. Villar, J. M. Corres, F. J. Arregui, and I. R. Matias, Sensors Actuators B **190**, 363 (2014).
15) Y. Zhao, L. Cai, X.-G. Li, F. Meng, and Z. Zhao, Sensors Actuator A **205**, 186 (2014).
16) P. Wang, G. Brambilla, M. Ding, Y. Semenova, Q. Wu, and G. Farrell, Opt. Lett. **36**, 2233 (2011).
17) X. Wang, K. Tian, L. Yuan, E. Lewis, G. Farrell, and P. Wang, J. Lightwave Technol. **36**, 2730 (2018).
18) A. Aitkulov and D. Tosi, IEEE Sens. J. **19**, 3282 (2019).
19) K. Wang, Y. Mizuno, X. Dong, W. Kurz, M. Fink, M. Jakobi, and A. W. Koch, Jpn. J. Appl. Phys. **61**, 078002 (2022).
20) A. A. Jasim, N. Hayashi, S. W. Harun, H. Ahmad, R. Penny, Y. Mizuno, and K. Nakamura, Sensors Actuator A **219**, 94 (2014).
21) A. Leal-Junior et al., Opt. Lett. **43**, 2539 (2018).
22) P. Xue, F. Yu, Y. Cao, and J. Zheng, IEEE Sens. J. **19**, 7434 (2019).
23) A. Leal-Junior et al., Opt. Express **26**, 12939 (2018).
24) C. A. F. Marques, D. J. Webb, and P. Andre, Opt. Fiber Technol. **36**, 144 (2017).
25) J. Huang, X. Lan, H. Wang, L. Yuan, T. Wei, Z. Gao, and H. Xiao, Opt. Lett. **37**, 4308 (2012).
26) G. Numata, N. Hayashi, M. Tabaru, Y. Mizuno, and K. Nakamura, IEEE Photon. J. **6**, 6802306 (2014).
27) G. Numata, N. Hayashi, M. Tabaru, Y. Mizuno, and K. Nakamura, Appl. Phys. Express **8**, 072502 (2015).
28) T. Kawa, G. Numata, H. Lee, N. Hayashi, Y. Mizuno, and K. Nakamura, Jpn. J. Appl. Phys. **56**, 078002 (2017).
29) A. Kumar, R. K. Varshney, S. Antony C, and P. Sharma, Opt. Commun. **219**, 215 (2003).
30) S. M. Tripathi, A. Kumar, R. K. Varshney, Y. B. P. Kumar, E. Marin, and J.-P. Meunier, J. Lightwave Technol. **27**, 2348 (2009).
31) Y. Koike and M. Asai, NPG Asia Mater. **1**, 22 (2009).